Supplementary information

Anionic and Cationic Redox Processes in β-Li_2IrO_3 and their Structural Implications on Electrochemical Cycling in Li-ion Cell

Paul E. Pearce[1,2,3,‡], Gaurav Assat[1,2,3,‡], Antonella Iadecola[2], François Fauth[4], Rémi Dedryvère[2,5], Artem Abakumov,[6] Gwenaëlle Rousse[1,2,3] and Jean-Marie Tarascon[1,2,3]*

[1]Collège de France, Chimie du Solide et de l'Energie, UMR 8260, 11 Place Marcelin Berthelot, 75231 Paris Cedex 05, France.
[2]Réseau sur le Stockage Electrochimique de l'Energie (RS2E), FR CNRS 3459, 80039 Amiens Cedex, France.
[3]Sorbonne Université, 4 Place Jussieu, F-75005 Paris, France.
[4]CELLS - ALBA synchrotron, Cerdanyola del Valles, Barcelona E-08290, Spain
[5]IPREM, CNRS, Université de Pau & Pays Adour, E2S-UPPA, Hélioparc, 2 Avenue P. Angot, 64053 Pau Cedex 9, France
[6]Skoltech Center for Energy Science and Technology, Skolkovo Institute of Science and Technology, Moscow 121205, Russian Federation

‡ These authors contributed equally.

* Correspondence with: jean-marie.tarascon@college-de-france.fr

Table S 1 Space group and unit cell parameters of the β-Li_xIrO_3 (x = 2, 1.5, 1, 0.5 and 0) phases as obtained from Rietveld refinement of the *operando* synchrotron X-ray powder diffraction data.

Composition	Space group	*a* (Å)	*b* (Å)	*c* (Å)	*β* (°)	Vol (Å^3)
Li_2IrO_3	*Fddd*	5.90709(7)	8.45673(9)	17.82779(16)	90	890.581(16)
$Li_{1.5}IrO_3$	*Fddd*	5.8279(3)	8.6685(4)	17.7380(9)	90	896.11(7)
Li_1IrO_3	*Fddd*	5.61885(6)	8.87546(9)	17.8926(3)	90	892.300(18)
$Li_{0.85}IrO_3$	*Fddd*	5.69115(15)	8.77962(17)	18.0435(4)	90	901.50(4)
$Li_{0.5}IrO_3$	*C*2/*c*	5.73738(20)	8.71946(19)	9.36504(18)	104.6815(14)	453.207(20)
IrO_3	*C*2/*c*	5.3493(4)	9.0662(3)	8.7203(4)	93.200(5)	422.26(4)
	*C*2/*c*	5.2822(4)	9.1414(4)	8.8473(5)	94.882(7)	425.66(4)

Table S 2 Crystallographic data and atomic positions of β-Li_2IrO_3 determined from Rietveld refinement of the *operando* synchrotron X-ray powder diffraction data. B*iso* was fixed to 1 for Li.

β-Li_2IrO_3

Space group *Fddd* R_{Bragg} = 6.83 % χ^2 = 10.91

a = 5.90709(7) Å *b* = 8.45673(9) Å *c* = 17.82779(16) Å V = 890.581(16) Å^3

Atom	Wyckoff position	*x/a*	*y/b*	*z/c*	Occupancy	B (Å^2)
Ir	16*g*	1/8	1/8	0.70824(8)	1	0.38(2)
Li1	16*g*	1/8	1/8	0.04167	1	1
Li2	16*g*	1/8	1/8	0.875	1	1
O1	16*e*	0.850(4)	1/8	1/8	1	0.64(14)
O2	32*h*	0.647(4)	0.3644(11)	0.0372(6)	1	0.64(14)

Table S 3 Crystallographic data and atomic positions of β-$Li_{1.5}IrO_3$ determined from Rietveld refinement of the *operando* synchrotron X-ray powder diffraction data. B_{iso} was fixed to 1 for O and Li.

β-$Li_{1.5}IrO_3$

Space group *F d d d* R_{Bragg} = 5.12 % χ^2 = 9.83

a = 5.8279(3) Å *b* = 8.6685(4) Å *c* = 17.7380(9) Å V = 896.11(7) Å^3

Atom	Wyckoff position	*x/a*	*y/b*	*z/c*	Occupancy	B (Å^2)
Ir	16*g*	1/8	1/8	0.70824(8)	1	0.38(2)
Li1	16*g*	1/8	1/8	0.04167	0.75	1
Li2	16*g*	1/8	1/8	0.875	0.75	1
O1	16*e*	0.850	1/8	1/8	1	1
O2	32*h*	0.647	0.3644	0.0372	1	1

Table S 4 Crystallographic data and atomic positions of β-Li_1IrO_3 determined from Rietveld refinement of the *operando* synchrotron X-ray powder diffraction data. B_{iso} was fixed to 1 for O and Li.

β-$LiIrO_3$

Space group *Fddd*			R_{Bragg} = 5.96 %		χ^2 = 12.1	
a = 5.61885(6) Å	*b* = 8.87546(9) Å	*c* = 17.8926(3) Å	V = 892.300(18) Å^3			
Atom	Wyckoff position	*x/a*	*y/b*	*z/c*	Occupancy	B (Å^2)
Ir	16*g*	1/8	1/8	0.70892(9)	1	0.50(2)
Li3	16*g*	1/8	0.973200	1/8	1	1
O1	16*e*	0.8566	1/8	1/8	1	1
O2	32*h*	0.6288	0.34651	0.03538	1	1

Table S 5 Crystallographic data and atomic positions of β-$Li_{0.85}IrO_3$ determined from Rietveld refinement of the *operando* synchrotron X-ray powder diffraction data. B_{iso} was fixed to 1 for O and Li.

β-$Li_{0.85}IrO_3$

Space group *Fddd*			R_{Bragg} = 8.74 %		χ^2 = 14.8	
a = 5.69115(15) Å	*b* = 8.77962(17) Å	*c* = 18.0435(4) Å	V = 901.50(4) Å^3			
Atom	Wyckoff position	*x/a*	*y/b*	*z/c*	Occupancy	B (Å^2)
Ir	16*g*	1/8	1/8	0.70788(10)	1	0.77(4)
Li3	16*g*	1/8	0.973200	1/8	0.85	1
O1	16*e*	0.8566	1/8	1/8	1	1
O2	32*h*	0.6288	0.34651	0.03538	1	1

Table S 6 Crystallographic data and atomic positions of β-$Li_{0.5}IrO_3$ determined from Rietveld refinement of the *operando* synchrotron X-ray powder diffraction data. B_{iso} was fixed to 1 for O and Li.

β-$Li_{0.5}IrO_3$

Space group *C2/c*			R_{Bragg} = 5.89 %		χ^2 = 10.00	
a = 5.73738(20) Å	*b* = 8.71946(19) Å	*c* = 9.36504(18) Å	β = 104.6815(14)°	V = 453.207(20) Å^3		
Atom	Wyckoff position	*x/a*	*y/b*	*z/c*	Occupancy	B (Å^2)
Ir	8*f*	0.0814(3)	0.3706(2)	0.41577(19)	1	0.46(3)
Li3b	4*c*	0.5	0.771910	0.75	1	1
O1	8*f*	0.208060	0.365940	0.245430	1	1
O2	8*f*	0.412510	0.094730	0.076140	1	1
O3	8*f*	0.094880	0.151200	0.449710	1	1

Table S 7 Crystallographic data and atomic positions of β-IrO_3 phase 1 determined from Rietveld refinement of the *operando* synchrotron X-ray powder diffraction data. B_{iso} was fixed to 1 for O.

β-IrO_3 phase 1

Space group *C*2/*c* R_{Bragg} = 6.56 % χ^2 = 4.29

a = 5.3493(4) Å *b* = 9.0662(3) Å *c* = 8.7203(4) Å β = 93.200(5)° V = 422.26(4) Å^3

Atom	Wyckoff position	*x/a*	*y/b*	*z/c*	Occupancy	B (Å^2)
Ir	8*f*	0.0883(7)	0.3645(3)	0.4171(3)	1	1.060(13)
O1	8*f*	0.208060	0.365940	0.245430	1	1
O2	8*f*	0.412510	0.094730	0.076140	1	1
O3	8*f*	0.094880	0.151200	0.449710	1	1

Table S 8 Crystallographic data and atomic positions of β-IrO_3 phase 2 determined from Rietveld refinement of the *operando* synchrotron X-ray powder diffraction data. B_{iso} was fixed to 1 for O.

β-IrO_3 phase 2

Space group *C*2/*c* R_{Bragg} = 4.53 % χ^2 = 4.29

a = 5.2822(4) Å *b* = 9.1414(4) Å *c* = 8.8473(5) Å β = 94.882(7)° V = 425.66(4) Å^3

Atom	Wyckoff position	*x/a*	*y/b*	*z/c*	Occupancy	B (Å^2)
Ir	8*f*	0.0720(9)	0.3697(5)	0.4231(4)	1	1.060(13)
O1	8*f*	0.208060	0.365940	0.245430	1	1
O2	8*f*	0.412510	0.094730	0.076140	1	1
O3	8*f*	0.094880	0.151200	0.449710	1	1

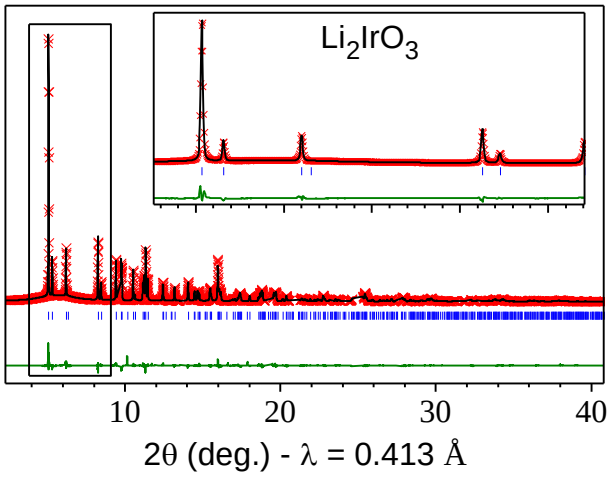

Figure S 1 Rietveld refinement of the *in situ* synchrotron X-ray powder diffraction patterns for β-Li_2IrO_3. In red are the experimental points, in black is the calculated pattern and in green is the difference between the experimental and calculated patterns. The vertical blue ticks beneath the pattern indicate the positions of the Bragg reflections.

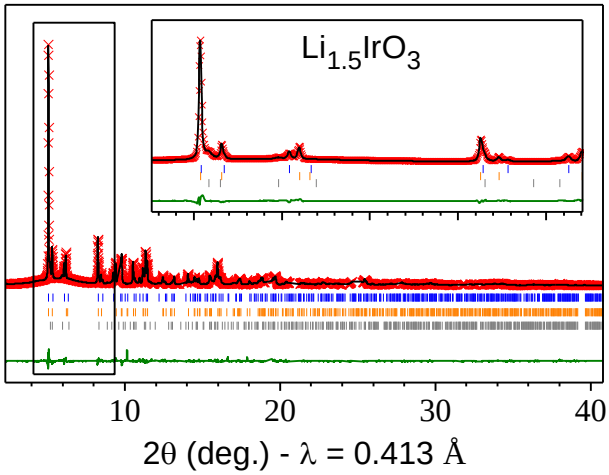

Figure S 2 Rietveld refinement of the *in situ* synchrotron X-ray powder diffraction patterns for β-$Li_{1.5}IrO_3$. In red are the experimental points, in black is the calculated pattern and in green is the difference between the experimental and calculated patterns. The vertical blue ticks beneath the pattern indicate the positions of the Bragg reflections. This refinement was carried out using three phases of composition x = 2, 1.5 and 1 which are shown by the blue, orange and grey ticks respectively.

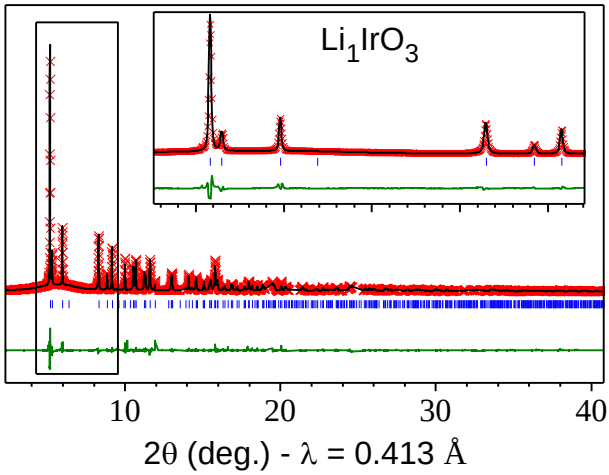

Figure S 3 Rietveld refinement of the *in situ* synchrotron X-ray powder diffraction patterns for β-Li_1IrO_3. In red are the experimental points, in black is the calculated pattern and in green is the difference between the experimental and calculated patterns. The vertical blue ticks beneath the pattern indicate the positions of the Bragg reflections.

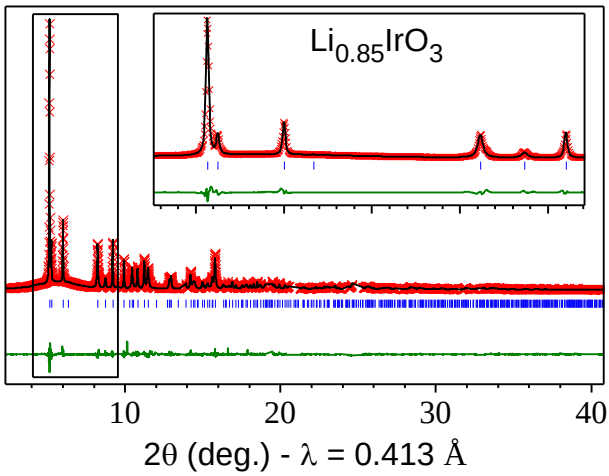

Figure S 4 Rietveld refinement of the *in situ* synchrotron X-ray powder diffraction patterns for β-$Li_{0.5}IrO_3$. In red are the experimental points, in black is the calculated pattern and in green is the difference between the experimental and calculated patterns. The vertical blue ticks beneath the pattern indicate the positions of the Bragg reflections.

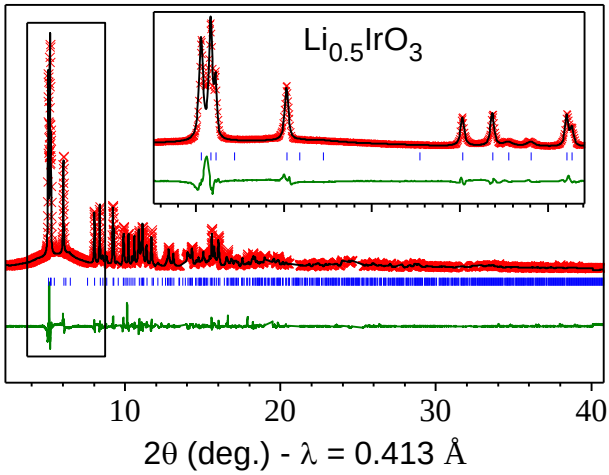

Figure S 5 Rietveld refinement of the *in situ* synchrotron X-ray powder diffraction patterns for β-$Li_{0.35}IrO_3$. In red are the experimental points, in black is the calculated pattern and in green is the difference between the experimental and calculated patterns. The vertical blue ticks beneath the pattern indicate the positions of the Bragg reflections.

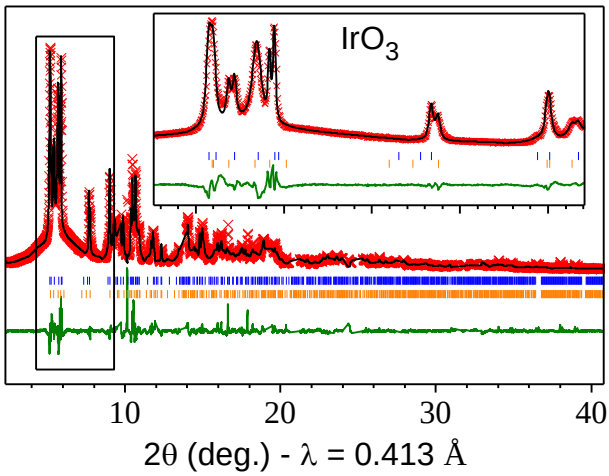

Figure S 6 Rietveld refinement of the *in situ* synchrotron X-ray powder diffraction patterns for β-IrO_3 which was only obtained as a mixture of two phases of compositions x = 0.35 and 0, in orange and blue respectively. In red are the experimental points, in black is the calculated pattern and in green is the difference between the experimental and calculated patterns. The vertical blue ticks beneath the pattern indicate the positions of the Bragg reflections. The blue and orange ticks correspond to the phases 2 and 1 respectively.

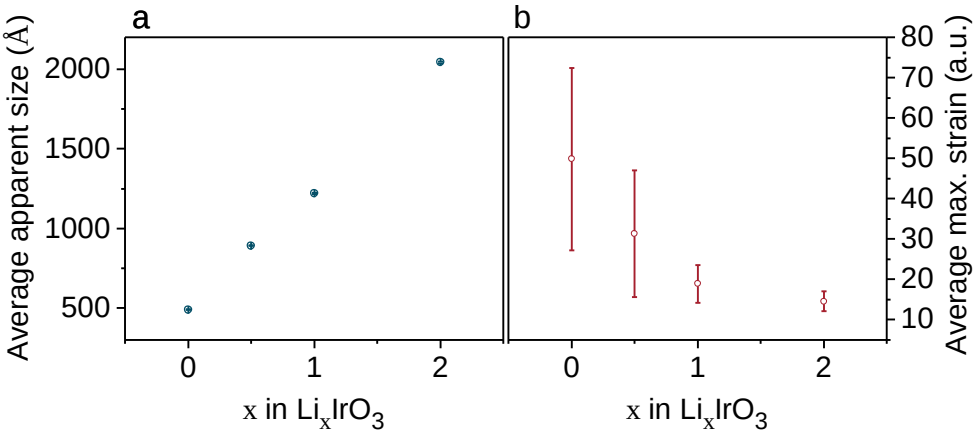

Figure S 7 Broadening parameters obtained from Rietveld refinements. a) The average apparent size which is determined by a lorentzian broadening varying in 1/cosθ. b) The average maximum strain obtained by both Gaussian and Lorentzian broadening varying in tanθ. The large standard deviation at high states of charge for the strain is due to its anisotropic nature.

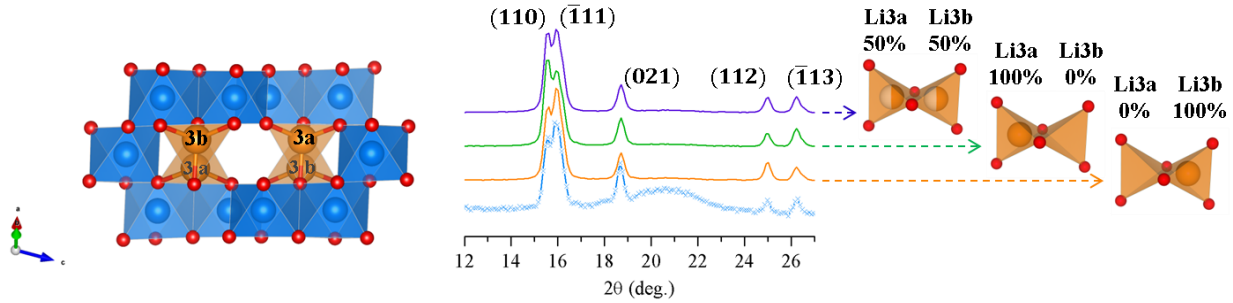

Figure S 8 Characteristic structure view (left) with Ir in blue, O in red and Li in orange. Experimental data in light blue, simulations for Li3b full and Li3a empty in orange, Li3a full and Li3b empty in green and both sites statistically filled in purple.

Table S 9 Crystallographic data and atomic positions of β-$Li_{0.5}IrO_3$ determined from Rietveld refinement of its neutron powder diffraction pattern.

β-$Li_{0.5}IrO_3$

Space group *C*2/*c* R_{Bragg} = 4.45 % χ^2 = 23.71

a = 5.7532(6) Å *b* = 8.6929(7) Å *c* = 9.3092(8) Å β = 104.604(5)° V = 450.53(7) Å^3

Atom	Wyckoff position	*x/a*	*y/b*	*z/c*	Occupancy	B (Å^2)
Ir	8*f*	0.0823(15)	0.3661(11)	0.4164(9)	1	1.33(14)
Li3b	4*c*	1/2	3/4	3/4	1	2(2)
O1	8*f*	0.2045(18)	0.365(2)	0.2451(10)	1	0.93(11)
O2	8*f*	0.402(2)	0.0937(15)	0.0751(13)	1	0.93(11)
O3	8*f*	0.091(2)	0.1484(19)	0.4509(12)	1	0.93(11)

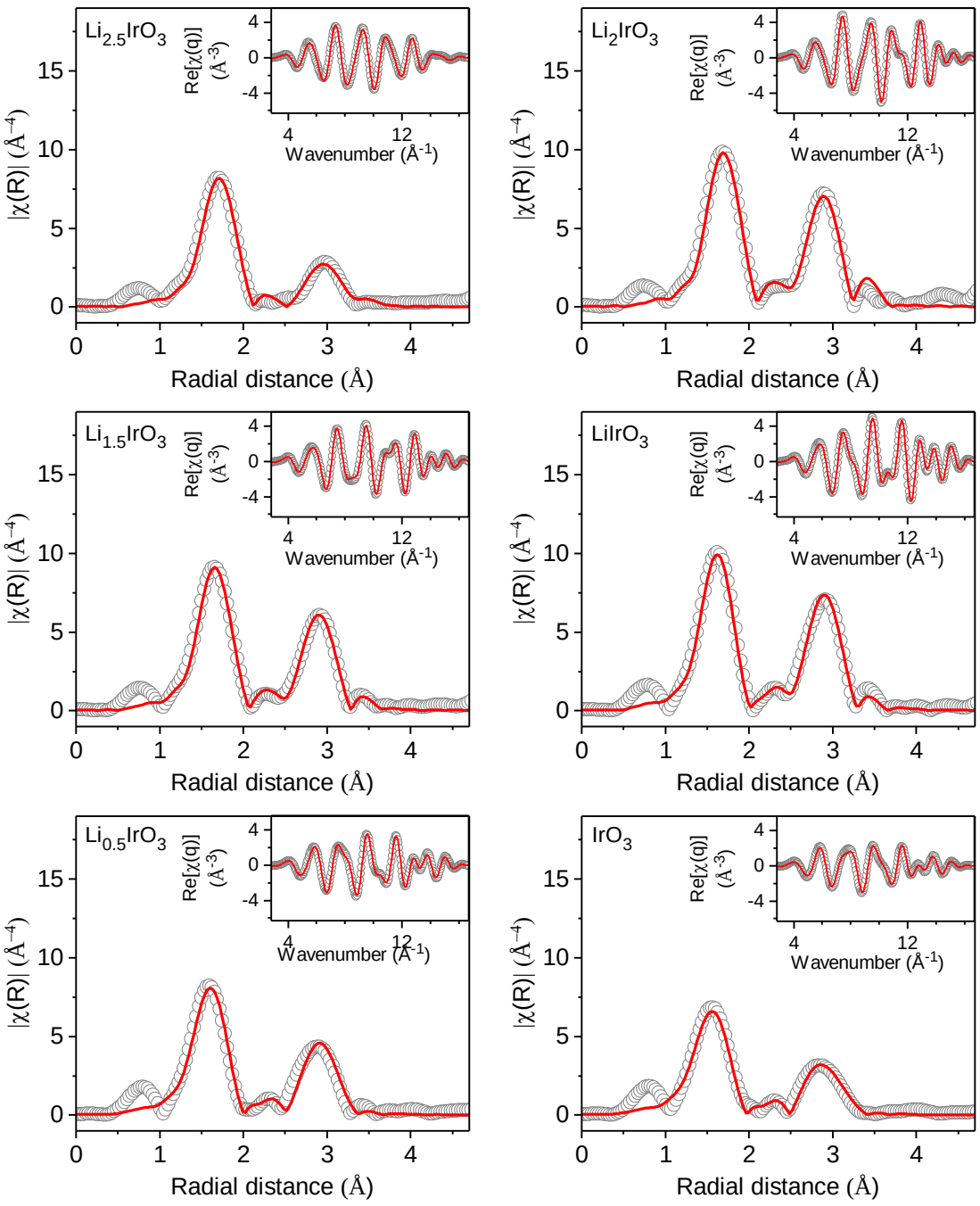

Figure S 9 Magnitude of the Fourier transform of k^3-weighted EXAFS oscillations for samples of compositions x = 2.5, 2, 1.5, 1, 0.5 and 0 (with x in Li_xIrO_3) along with the fitting results in both R- and q-space (The |χ(R)| plots were not corrected for phase shifts).

Table S 10 Fitting results of EXAFS measured on ex situ samples at different lithium contents for β-Li_2IrO_3.

x	IrO_6 (first shell)			$IrIr_3$ (second shell)			Calculated O-O distance (Å)
	CN	*R* (Å)	σ^2 (Å^2)	CN	*R* (Å)	σ^2 (Å^2)	
2.5	6	2.054 (2)	0.0033 (2)	3	3.047 (4)	0.0068 (3)	2.754 (4) R-factor = 0.0118
2	6	2.033 (1)	0.0024 (1)	3	2.998 (1)	0.00291 (8)	2.746 (2) R-factor = 0.0031
1.5	6	2.006 (2)	0.0030 (2)	3	3.010 (1)	0.0035 (1)	2.652 (2) R-factor = 0.0040
1	6	1.968 (2)	0.0026 (2)	3	3.018 (2)	0.0026 (1)	2.528 (3) R-factor = 0.0077
0.5	6	1.958 (1)	0.0039 (5)	3	3.034 (3)	0.0043 (3)	2.476 (3) R-factor = 0.0160
0	6	1.930 (2)	0.005 (2)	3	3.030 (2)	0.0053 (2)	2.391 (3) R-factor = 0.0164

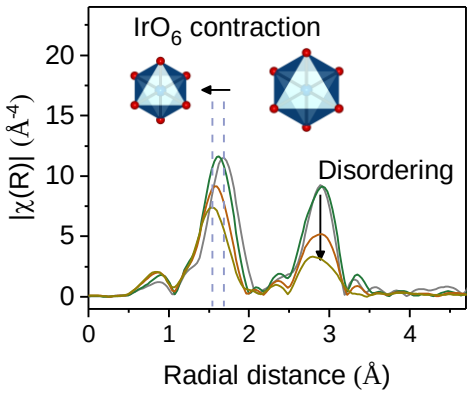

Figure S 10 Magnitude of the Fourier transform of k^3-weighted EXAFS oscillations for samples of compositions *x* = 2.5, 2, 1.5, 1, 0.5 and 0 (with *x* in Li_xIrO_3) showing the shift in the first shel and the broadening of the peaks.

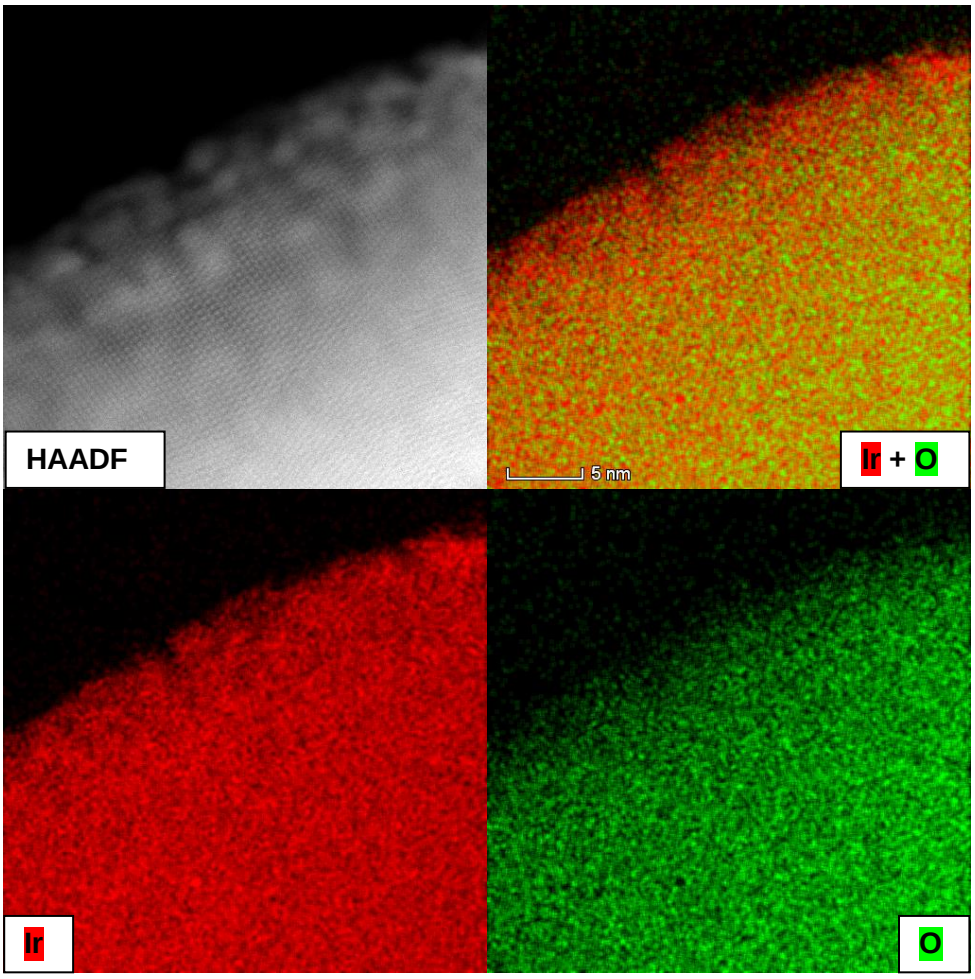

Figure S 11 HAADF-STEM image, Ir and O EDX compositional maps and the color-coded mixed map of the surface nanoclusters in the sample cycled between 2.0 - 4.8 V.